Physics Letters A 377 (2013) 3247–3253

Contents lists available at ScienceDirect

Physics Letters A

www.elsevier.com/locate/pla

Tachyonic Cherenkov emission from Jupiter's radio electrons

Roman Tomaschitz

Department of Physics, Hiroshima University, 1-3-1 Kagami-yama, Higashi-Hiroshima 739-8526, Japan

ARTICLE INFO

Article history:
Received 29 September 2013
Accepted 11 October 2013
Available online 17 October 2013
Communicated by V.M. Agranovich

Keywords:
Tachyonic Cherenkov radiation
Superluminal radiation modes with negative mass-square
Transversal and longitudinal tachyons
Tachyonic Maxwell–Proca fields in a permeable spacetime
Thermal electron plasma in Jupiter's radiation belts
Cassini's Jupiter fly-by and Jovian radio spectrum

ABSTRACT

Tachyonic Cherenkov radiation from inertial relativistic electrons in the Jovian radiation belts is studied. The tachyonic modes are coupled to a frequency-dependent permeability tensor and admit a negative mass-square, rendering them superluminal and dispersive. The superluminal radiation field can be cast into Maxwellian form, using 3D field strengths and inductions, and the spectral densities of tachyonic Cherenkov radiation are derived. The negative mass-square gives rise to a longitudinal flux component. A spectral fit to Jupiter's radio spectrum, inferred from ground-based observations and the Cassini 2001 fly-by, is performed with tachyonic Cherenkov flux densities averaged over a thermal electron population.

1. Introduction

During the Cassini Jupiter fly-by in January 2001, an in situ measurement of the Jovian radio emission was performed, resulting in an unexpectedly low flux density of 0.44 ± 0.15 Jy at 13.8 GHz [1], as compared to ground-based observations at 8.6 GHz [2], which produced an averaged flux of 2.3 ± 0.6 Jy. This sudden decline is hard to explain with magnetospheric ultra-relativistic synchrotron radiation models. Here, we investigate the presently available radio spectrum ranging from 74 MHz up to the Cassini flux at 13.8 GHz. We perform a spectral fit to the Jovian radio flux with a tachyonic Cherenkov density [3–6] produced by mildly relativistic thermal electrons in the radiation belts. The superluminal radiation field (Proca field) satisfies Maxwell's equations with negative mass-square [7]. On that basis, we derive the tachyonic Cherenkov flux generated by inertial charges propagating in a dispersive spacetime.

In Section 2, we discuss Proca fields with negative mass-square and frequency-dependent permeabilities. We outline the tachyonic Maxwell equations in terms of 3D field strengths and inductions and develop the 4D Lagrange formalism using dispersive permeability tensors. We obtain field equations which have a manifestly covariant appearance, even though the permeability tensors are a manifestation of the absolute spacetime required for causal superluminal signal transfer [8–10].

In Section 3, we analyze asymptotic tachyonic radiation fields generated by a classical subluminal current density, and decompose them into transversal and longitudinal field components. In Section 4, we derive the tachyonic Cherenkov flux densities of a relativistic charge in uniform motion. A longitudinal radiation component emerges whose intensity scales with the negative mass-square of the radiation field. As in the case of electromagnetic Cherenkov radiation, the mass of the radiating particle does not enter in the tachyonic Cherenkov densities. This gives credence to the view [3], that Cherenkov radiation is not so much radiation by a charge passing through a medium, but rather radiation by the medium itself, excited by the field of the inertial charge.

In Section 5, we average the differential tachyonic Cherenkov flux over relativistic electron distributions (thermal Maxwell–Boltzmann and nonthermal power-law distributions). In Section 6.1, we discuss spectral fitting with Cherenkov flux densities, adapted to Jupiter's radio band. In Section 6.2, a spectral fit to the Jovian radio emission is performed. The low flux density at 13.8 GHz measured by the Cassini spacecraft can well be explained by tachyonic Cherenkov emission from thermal electrons in Jupiter's radiation belts, the Cassini data point being located in the exponentially decaying spectral tail. In Section 7, we present our conclusions.

E-mail address: tom@geminga.org.

0375-9601/$ – see front matter
http://dx.doi.org/10.1016/j.physleta.2013.10.016

2. Tachyonic Proca–Maxwell fields: manifestly covariant field equations in a permeable spacetime

We start with some conventions regarding the Fourier time transform. The vector potential $A_\mu = (A_0, \mathbf{A})$ transforms as $\hat{A}_\mu(\mathbf{x},\omega) = \int_{-\infty}^{\infty} A_\mu(\mathbf{x},t)\mathrm{e}^{\mathrm{i}\omega t}\,\mathrm{d}t$, and the same holds for the field strengths, inductions and the current. Since A_μ is real, $\hat{A}^*_\mu(\mathbf{x},\omega) = \hat{A}_\mu(\mathbf{x},-\omega)$. The homogeneous Maxwell equations in space–frequency representation read $\operatorname{rot}\hat{\mathbf{E}} - \mathrm{i}\omega\hat{\mathbf{B}} = 0$, $\operatorname{div}\hat{\mathbf{B}} = 0$. The field strengths $\hat{\mathbf{E}}(\mathbf{x},\omega)$ and $\hat{\mathbf{B}}(\mathbf{x},\omega)$ are related to the vector potential by $\hat{\mathbf{E}} = \mathrm{i}\omega\hat{\mathbf{A}} + \nabla\hat{A}_0$, $\hat{\mathbf{B}} = \operatorname{rot}\hat{\mathbf{A}}$. The constitutive equations defining the inductions $\hat{\mathbf{D}}$ and $\hat{\mathbf{H}}$ and the inductive potential $\hat{C}_\mu = (\hat{C}_0, \hat{\mathbf{C}})$ read [7,11]

$$\hat{\mathbf{D}}(\mathbf{x},\omega) = \varepsilon(\omega)\hat{\mathbf{E}}(\mathbf{x},\omega), \qquad \hat{\mathbf{B}}(\mathbf{x},\omega) = \mu(\omega)\hat{\mathbf{H}}(\mathbf{x},\omega),$$
$$\hat{\mathbf{A}}(\mathbf{x},\omega) = \mu_0(\omega)\hat{\mathbf{C}}(\mathbf{x},\omega), \qquad \hat{C}_0(\mathbf{x},\omega) = \varepsilon_0(\omega)\hat{A}_0(\mathbf{x},\omega). \tag{2.1}$$

The permeabilities $\varepsilon(\omega)$, $\mu(\omega)$, $\mu_0(\omega)$ and $\varepsilon_0(\omega)$ are independent of the space variable, real and symmetric $\varepsilon(\omega) = \varepsilon(-\omega)$. The inhomogeneous field equations coupled to a current $\hat{j}^\mu_\Omega = (\hat{\rho}_\Omega, \hat{\mathbf{j}}_\Omega)$ (which will be defined in (2.5)) read

$$\operatorname{rot}\hat{\mathbf{H}} + \mathrm{i}\omega\hat{\mathbf{D}} = \hat{\mathbf{j}}_\Omega + m_\mathrm{t}^2(\omega)\hat{\mathbf{C}}, \qquad \operatorname{div}\hat{\mathbf{D}} = \hat{\rho}_\Omega - m_\mathrm{t}^2(\omega)\hat{C}_0. \tag{2.2}$$

$m_\mathrm{t}^2(\omega)$ is the negative tachyonic mass-square ($m_\mathrm{t}^2 > 0$ in our sign convention), which can be frequency-dependent like the permeabilities, $m_\mathrm{t}^2(\omega) = m_\mathrm{t}^2(-\omega)$. We take the divergence of the first equation in (2.2) and substitute the second, to obtain the Lorentz condition $\operatorname{div}\hat{\mathbf{C}} + \mathrm{i}\omega\hat{C}_0 = 0$, subject to current conservation $\mathrm{i}\omega\hat{\rho}_\Omega - \operatorname{div}\hat{\mathbf{j}}_\Omega = 0$. The corresponding Fourier representation of the Poynting flux vector [11] is $\hat{\mathbf{S}} = \hat{\mathbf{E}}\times\hat{\mathbf{H}}^* + m_\mathrm{t}^2\hat{A}_0\hat{\mathbf{C}}^* + \text{c.c.}$

To write the Maxwell equations manifestly covariantly in Fourier space, we start with the field tensor $F_{\mu\nu}(\mathbf{x},t) = A_{\nu,\mu} - A_{\mu,\nu}$. We use the convention that time differentiation in Fourier space means to multiply with a factor $-\mathrm{i}\omega$, e.g. $\hat{A}_{\mu,0}(\mathbf{x},\omega) = -\mathrm{i}\omega\hat{A}_\mu$. For conjugated fields, $\hat{A}^*_{\mu,0} = \mathrm{i}\omega\hat{A}^*_\mu$. Thus, $\hat{F}_{\mu\nu}(\mathbf{x},\omega) = \hat{A}_{\nu,\mu} - \hat{A}_{\mu,\nu}$ and $\hat{j}^\mu_{\Omega,\mu} = 0$, which actually means $\hat{j}^m_{\Omega,m} - \mathrm{i}\omega\hat{j}^0_\Omega = 0$. The 3D field strengths are $\hat{E}_k = \hat{F}_{k0}$ and $\hat{B}^k = \varepsilon^{kij}\hat{F}_{ij}/2 = \varepsilon^{kij}\hat{A}_{j,i}$, and inversely $\hat{F}_{ij} = \varepsilon_{ijk}\hat{B}^k$, where ε^{kij} is the Levi-Civita 3-tensor. The manifestly covariant homogeneous field equations read $\varepsilon^{\kappa\lambda\mu\nu}\hat{F}_{\mu\nu,\lambda} = 0$, where $\varepsilon^{\kappa\lambda\mu\nu}$ is the totally antisymmetric 4-tensor.

The permeabilities $(\varepsilon_0(\omega), \mu_0(\omega))$ and $(\varepsilon(\omega), \mu(\omega))$ in (2.1) define isotropic real and symmetric permeability tensors $g_A^{\mu\nu}(\omega)$ and $g_F^{\mu\nu}(\omega)$ [7],

$$g_A^{00} = -\varepsilon_0, \qquad g_A^{ij} = \frac{\delta^{ij}}{\mu_0},$$
$$g_F^{00} = -\mu^{1/2}\varepsilon, \qquad g_F^{ij} = \frac{\delta^{ij}}{\mu^{1/2}}, \tag{2.3}$$

with zero flanks $g_{A,F}^{0i} = 0$ and $g_{A,F}^{\mu\nu}(\omega) = g_{A,F}^{\mu\nu}(-\omega)$. Greek indices are raised and lowered with the Minkowski metric $\eta_{\mu\nu} = \operatorname{diag}(-1,1,1,1)$. We may then write the inductions (2.1) manifestly covariantly as $\hat{C}^\mu = g_A^{\mu\nu}\hat{A}_\nu$, $\hat{H}^{\alpha\beta} = g_F^{\alpha\mu}g_F^{\beta\nu}\hat{F}_{\mu\nu}$, so that $\hat{D}^l = \hat{H}^{0l} = \varepsilon\hat{E}^l$ and $\hat{H}_i = \varepsilon_{ikl}\hat{H}^{kl}/2 = \hat{B}_i/\mu$, and inversely $\hat{H}^{mn} = \hat{H}_j\varepsilon^{jmn}$. Also, $\hat{H}^{kl} = \hat{F}_{kl}/\mu$ and $\hat{H}^{0l} = -\varepsilon\hat{F}_{0l}$.

The action functional is $S = (2\pi)^{-1}\int\hat{L}(\mathbf{x},\omega)\,\mathrm{d}\mathbf{x}\,\mathrm{d}\omega$, defined by the Lagrangian

$$\hat{L} = -\frac{1}{4}\hat{F}_{\alpha\beta}g_F^{\alpha\mu}g_F^{\beta\nu}\hat{F}_{\mu\nu} + \frac{1}{2}m_\mathrm{t}^2\hat{A}_\mu g_A^{\mu\nu}\hat{A}_\nu + \hat{A}_\mu g_J^{\mu\nu}\hat{j}_\nu$$
$$= -\frac{1}{4}\hat{F}_{\mu\nu}\hat{H}^{\mu\nu} + \frac{1}{2}m_\mathrm{t}^2\hat{A}_\mu\hat{C}^\mu + \hat{A}_\mu\hat{j}^\mu_\Omega. \tag{2.4}$$

The coupling of the wave modes to an external current $\hat{j}_\nu(\mathbf{x},\omega)$ is effected by a permeability tensor $g_J^{\mu\nu}(\omega)$,

$$g_J^{00} = -\Omega_0(\omega), \qquad g_J^{mn} = \frac{\delta^{mn}}{\Omega(\omega)}, \qquad g_J^{k0} = 0, \tag{2.5}$$

with the same properties as the tensors $g_{A,F}^{\mu\nu}$ in (2.3). In the field equations (2.2), we use the 'dressed' current $\hat{j}^\mu_\Omega = g_J^{\mu\nu}\hat{j}_\nu = (\hat{\rho}_\Omega, \hat{\mathbf{j}}_\Omega)$. Euler variation of the action gives the manifestly covariant field equations $\hat{H}^{\mu\nu}{}_{,\nu} - m_\mathrm{t}^2\hat{C}^\mu = \hat{j}^\mu_\Omega$ in space–frequency $(\mathbf{x},\omega)$ representation, equivalent to (2.2). ($\hat{H}^{m0}{}_{,0}(\mathbf{x},\omega) = -\mathrm{i}\omega\hat{H}^{m0}$, as defined above.) If the current $\hat{j}^\mu_\Omega$ is conserved, $\hat{j}^\mu_{\Omega,\mu} = 0$, we find the Lorentz condition $\hat{C}^\mu{}_{,\mu} = 0$. The permeability tensor (2.5) amounts to a frequency-dependent coupling constant in Lagrangian (2.4) if $\Omega_0(\omega) = 1/\Omega(\omega)$, which we assume in the following, $\hat{j}^\mu_\Omega = \hat{j}^\mu/\Omega(\omega)$. Thus, if the external current is conserved, $\hat{j}^m{}_{,m} - \mathrm{i}\omega\hat{j}^0 = 0$, this also holds for the dressed current $\hat{j}^\mu_\Omega$. In fact, $\Omega(\omega)$ can be scaled into the permeabilities (2.1), $\varepsilon\to\Omega\varepsilon$, $\mu\to\mu/\Omega$, and analogously for (ε_0,μ_0), cf. (2.2).

3. Asymptotic radiation fields: time-averaged transversal and longitudinal energy flux

The tachyonic Maxwell equations (stated in (2.2) and after (2.5), with permeability tensors in (2.3) and (2.5)) are solved by the transversal and longitudinal asymptotic vector potentials [12,13]

$$\hat{\mathbf{A}}^{\mathrm{T,L}}(\mathbf{x},\omega) \sim \frac{1}{\Omega}\frac{\lambda^{\mathrm{T,L}}}{4\pi r}\mathrm{e}^{\mathrm{i}k_{\mathrm{T,L}}r}\int\mathrm{e}^{-\mathrm{i}k_{\mathrm{T,L}}\mathbf{n}\mathbf{x}'}\hat{\mathbf{j}}^{\mathrm{T,L}}\big(\mathbf{x}',\omega\big)\,\mathrm{d}\mathbf{x}'. \tag{3.1}$$

Here, we substitute the transversal/longitudinal current components, defined with the radial unit wave vector $\mathbf{n} = \mathbf{x}/r$: $\mathbf{n}\hat{\mathbf{j}}^\mathrm{T} = 0$ and $\mathbf{n}\times\hat{\mathbf{j}}^\mathrm{L} = 0$. We also note $\operatorname{div}\hat{\mathbf{A}}^\mathrm{T} = \mathrm{O}(1/r^2)$ and $\operatorname{rot}\hat{\mathbf{A}}^\mathrm{L} = \mathrm{O}(1/r^2)$. $\lambda^{\mathrm{T,L}}$ in (3.1) stands for $\lambda^\mathrm{T} = \mu$, $\lambda^\mathrm{L} = \varepsilon_0\mu_0/\varepsilon$, and the wave numbers $k_{\mathrm{T,L}}$ are defined by the dispersion relations $k_{\mathrm{T,L}} = \operatorname{sign}(\omega)\kappa_{\mathrm{T,L}}(\omega)$, where [14]

$$\kappa_\mathrm{T}^2 = \varepsilon\mu\omega^2 + m_\mathrm{t}^2\frac{\mu}{\mu_0}, \qquad \kappa_\mathrm{L}^2 = \varepsilon_0\mu_0\omega^2 + m_\mathrm{t}^2\frac{\varepsilon_0}{\varepsilon}, \tag{3.2}$$

and $k_\mathrm{L}^2 = k_\mathrm{T}^2\varepsilon_0\mu_0/(\varepsilon\mu)$. It is convenient to define the current transform [15]

$$\hat{\mathbf{j}}(\mathbf{x},\omega,k_{\mathrm{T,L}}) = \int\mathrm{d}\mathbf{x}'\,\hat{\mathbf{j}}\big(\mathbf{x}',\omega\big)\exp\big(-\mathrm{i}k_{\mathrm{T,L}}(\omega)\mathbf{n}\mathbf{x}'\big), \tag{3.3}$$

whose transversal and longitudinal projections read

$$\hat{\mathbf{j}}^\mathrm{T}(\mathbf{x},\omega) = \hat{\mathbf{j}}(\mathbf{x},\omega,k_\mathrm{T}) - \mathbf{n}\big(\mathbf{n}\hat{\mathbf{j}}(\mathbf{x},\omega,k_\mathrm{T})\big),$$
$$\hat{\mathbf{j}}^\mathrm{L}(\mathbf{x},\omega) = \mathbf{n}\big(\mathbf{n}\hat{\mathbf{j}}(\mathbf{x},\omega,k_\mathrm{L})\big), \tag{3.4}$$

so that the integral in (3.1) can be replaced by $\hat{\mathbf{j}}^{\mathrm{T,L}}(\mathbf{x},\omega)$.

The transversal field strengths read $\hat{\mathbf{E}}^\mathrm{T}(\mathbf{x},\omega) = \mathrm{i}\omega\hat{\mathbf{A}}^\mathrm{T}$, $\hat{\mathbf{B}}^\mathrm{T} = \operatorname{rot}\hat{\mathbf{A}}^\mathrm{T}$, $\hat{A}^\mathrm{T}_0 = 0$, and the longitudinal ones are $\hat{\mathbf{E}}^\mathrm{L} \sim m_\mathrm{t}^2\hat{\mathbf{A}}^\mathrm{L}/(\mathrm{i}\omega\mu_0\varepsilon)$, $\hat{\mathbf{B}}^\mathrm{L} = 0$ and $\hat{A}^\mathrm{L}_0 = -\operatorname{div}\hat{\mathbf{A}}^\mathrm{L}/(\mathrm{i}\omega\varepsilon_0\mu_0)$. The polarization components $\hat{\mathbf{S}}^{\mathrm{T,L}}(\mathbf{x},\omega)$ of the energy flux vector can thus be assembled as, cf. after (2.2),

$$\hat{\mathbf{S}}^\mathrm{T} \sim \hat{\mathbf{E}}^\mathrm{T}\times\hat{\mathbf{H}}^* + \text{c.c.} \sim \frac{2\mu\omega k_\mathrm{T}}{(4\pi r\Omega)^2}\mathbf{n}\big(\hat{\mathbf{j}}^\mathrm{T}(\mathbf{x},\omega)\hat{\mathbf{j}}^{\mathrm{T}*}(\mathbf{x},\omega)\big),$$
$$\hat{\mathbf{S}}^\mathrm{L} \sim -m_\mathrm{t}^2\hat{A}_0\hat{\mathbf{C}}^{\mathrm{L}*} + \text{c.c.} \sim \frac{2m_\mathrm{t}^2}{(4\pi r\Omega)^2}\frac{\varepsilon_0}{\varepsilon^2}\frac{k_\mathrm{L}}{\omega}\mathbf{n}\big(\hat{\mathbf{j}}^\mathrm{L}(\mathbf{x},\omega)\hat{\mathbf{j}}^{\mathrm{L}*}(\mathbf{x},\omega)\big). \tag{3.5}$$

We perform a time average (also see (4.1) below),

$$\langle \mathbf{S}^{\mathrm{T}} \rangle = \frac{1}{T} \int_{-T/2}^{+T/2} \mathbf{E}^{\mathrm{T}}(\mathbf{x},t) \times \mathbf{H}(\mathbf{x},t)\,\mathrm{d}t,$$

$$\langle \mathbf{S}^{\mathrm{L}} \rangle = -\frac{m_{\mathrm{t}}^2}{T} \int_{-T/2}^{+T/2} A_0(\mathbf{x},t)\mathbf{C}^{\mathrm{L}}(\mathbf{x},t)\,\mathrm{d}t, \tag{3.6}$$

to find

$$\langle \mathbf{S}^{\mathrm{T}} \rangle \sim \frac{1}{2\pi T} \frac{\mathbf{n}}{(4\pi r)^2} \int_{-\infty}^{+\infty} \frac{\mu\omega k_{\mathrm{T}}}{\Omega^2} \big(\hat{\mathbf{J}}^{\mathrm{T}}(\mathbf{x},\omega)\hat{\mathbf{J}}^{\mathrm{T}*}(\mathbf{x},\omega)\big)\,\mathrm{d}\omega,$$

$$\langle \mathbf{S}^{\mathrm{L}} \rangle \sim \frac{m_{\mathrm{t}}^2}{2\pi T} \frac{\mathbf{n}}{(4\pi r)^2} \int_{-\infty}^{+\infty} \frac{\varepsilon_0 k_{\mathrm{L}}}{\varepsilon^2\Omega^2\omega} \big(\hat{\mathbf{J}}^{\mathrm{L}}(\mathbf{x},\omega)\hat{\mathbf{J}}^{\mathrm{L}*}(\mathbf{x},\omega)\big)\,\mathrm{d}\omega, \tag{3.7}$$

from which the transversal and longitudinal Cherenkov flux densities can be extracted, cf. Section 4.

4. Superluminal radiation by an inertial charge in a dispersive spacetime

We consider a classical point charge q in uniform motion $\mathbf{x}_0(t) = \boldsymbol{\upsilon} t$, with subluminal speed $\upsilon < 1$. The charge and current densities are $\rho = q\delta(\mathbf{x} - \boldsymbol{\upsilon} t)$ and $\mathbf{j}(\mathbf{x},t) = q\boldsymbol{\upsilon}\delta(\mathbf{x} - \boldsymbol{\upsilon} t)$. We use the Heaviside–Lorentz system, so that $\alpha_{\mathrm{e}} = e^2/(4\pi\hbar c) \approx 1/137$ and $\alpha_{\mathrm{q}} = q^2/(4\pi\hbar c)$ are the electric and tachyonic fine-structure constants. The current transform (3.3) reads

$$\hat{\mathbf{J}}(\mathbf{x},\omega,k_{\mathrm{T,L}};T) = q\boldsymbol{\upsilon} \int_{-T/2}^{+T/2} \exp\big[-\mathrm{i}\big(k_{\mathrm{T,L}}(\omega)\mathbf{n}\boldsymbol{\upsilon} - \omega\big)t\big]\,\mathrm{d}t, \tag{4.1}$$

where the time cutoff $T \to \infty$ has been introduced as a regularization. The time integration is performed by means of the limit definition $\delta_{(1),T}(\omega) = (2\pi)^{-1}\int_{-T/2}^{+T/2} \mathrm{e}^{\mathrm{i}\omega t}\,\mathrm{d}t$ of the Dirac function. A second limit definition, $\delta_{(2),T}(\omega) = (2\pi/T)\delta_{(1),T}^2(\omega)$, is invoked in (4.2) to calculate the time-averaged flux vectors. We write $\hat{\mathbf{J}}(\mathbf{x},\omega,k_{\mathrm{T,L}};T) = 2\pi q\boldsymbol{\upsilon}\delta_{(1),T}(\omega - k_{\mathrm{T,L}}(\omega)\mathbf{n}\boldsymbol{\upsilon})$ and use $\boldsymbol{\upsilon}$ as polar axis, $\mathbf{n}\boldsymbol{\upsilon} = \upsilon\cos\theta$, to find, cf. (3.7),

$$\langle \mathbf{S}^{\mathrm{T}} \rangle \sim \frac{q^2\upsilon^2\mathbf{n}}{(4\pi r)^2} \sin^2\theta \int_{-\infty}^{+\infty} \frac{\mu\omega k_{\mathrm{T}}}{\Omega^2} \delta_{(2),T}\big(k_{\mathrm{T}}(\omega)\upsilon\cos\theta - \omega\big)\,\mathrm{d}\omega,$$

$$\langle \mathbf{S}^{\mathrm{L}} \rangle \sim \frac{q^2\upsilon^2 m_{\mathrm{t}}^2\mathbf{n}}{(4\pi r)^2} \cos^2\theta \int_{-\infty}^{+\infty} \frac{\varepsilon_0 k_{\mathrm{L}}}{\omega\varepsilon^2\Omega^2} \delta_{(2),T}\big(k_{\mathrm{L}}(\omega)\upsilon\cos\theta - \omega\big)\,\mathrm{d}\omega. \tag{4.2}$$

Performing the limit $T \to \infty$, we can replace $\delta_{(2),T}$ by the ordinary delta function.

The radiant transversal/longitudinal power is obtained by integrating the Poynting vectors (4.2) over a sphere of radius $r \to \infty$, $P^{\mathrm{T,L}} = r^2 \int \langle \mathbf{S}^{\mathrm{T,L}} \rangle \mathbf{n} \sin\theta\,\mathrm{d}\theta\,\mathrm{d}\varphi$. By interchanging the $\mathrm{d}\theta$ and $\mathrm{d}\omega$ integrations, we find

$$P^{\mathrm{T}} = \int_0^{\omega_{\mathrm{T,max}}} p^{\mathrm{T}}(\omega)\,\mathrm{d}\omega, \qquad P^{\mathrm{L}} = \int_0^{\omega_{\mathrm{L,max}}} p^{\mathrm{L}}(\omega)\,\mathrm{d}\omega, \tag{4.3}$$

where $p^{\mathrm{T,L}}(\omega)$ are the tachyonic Cherenkov densities for transversal/longitudinal radiation,

$$p^{\mathrm{T}}(\omega) = \frac{q^2\upsilon}{4\pi} \frac{\mu(\omega)\omega}{\Omega^2(\omega)} \bigg(1 - \frac{\omega^2}{k_{\mathrm{T}}^2(\omega)\upsilon^2}\bigg),$$

$$p^{\mathrm{L}}(\omega) = \frac{q^2}{4\pi\upsilon} \frac{m_{\mathrm{t}}^2(\omega)\varepsilon_0(\omega)}{\varepsilon^2(\omega)\Omega^2(\omega)} \frac{\omega}{k_{\mathrm{L}}^2(\omega)}. \tag{4.4}$$

The integration range in (4.3) is actually over positive ω intervals in which $\omega/(k_{\mathrm{T,L}}(\omega)\upsilon) \leqslant 1$, cf. (3.2). From now on, we will use constant (i.e. frequency-independent) permeabilities (ε,μ) and (ε_0,μ_0) as well as a constant tachyonic mass-square m_{t}^2. In this case, the integration range in (4.3) is defined by cutoff frequencies $\omega_{\mathrm{T,L,max}}$ obtained as the solutions of $k_{\mathrm{T,L}}(\omega)\upsilon = \omega$, respectively.

In the tachyonic spectral densities (4.4), we substitute the wave numbers (3.2), and parametrize the particle velocity with the Lorentz factor, $\upsilon = \sqrt{\gamma^2-1}/\gamma$:

$$p^{\mathrm{T}}(\omega,\gamma) = \frac{q^2}{4\pi} \frac{m_{\mathrm{t}}^2\mu}{\Omega^2} \frac{\omega}{\varepsilon\mu_0\omega^2 + m_{\mathrm{t}}^2} \bigg(1 - \frac{1}{\eta_{\mathrm{T}}(\gamma)} \frac{\omega^2}{m_{\mathrm{t}}^2}\bigg) \frac{\sqrt{\gamma^2-1}}{\gamma},$$

$$p^{\mathrm{L}}(\omega,\gamma) = \frac{q^2}{4\pi} \frac{m_{\mathrm{t}}^2}{\varepsilon\Omega^2} \frac{\omega}{\varepsilon\mu_0\omega^2 + m_{\mathrm{t}}^2} \frac{\gamma}{\sqrt{\gamma^2-1}}, \tag{4.5}$$

where we use the shortcut

$$\eta_{\mathrm{T}}(\gamma) = \frac{1}{\varepsilon\mu_0} \frac{\gamma^2-1}{1 + (1/(\varepsilon\mu) - 1)\gamma^2}. \tag{4.6}$$

We also define $\eta_{\mathrm{L}}(\gamma)$ analogous to $\eta_{\mathrm{T}}(\gamma)$ with the product $\varepsilon\mu$ in (4.6) replaced by $\varepsilon_0\mu_0$. In the following, we restrict to permeabilities satisfying $\varepsilon\mu \leqslant 1$ and $\varepsilon_0\mu_0 \leqslant 1$, since the spectral averaging carried out in the next section leads to exponentially decaying spectral densities only in this case. Subject to these constraints, the functions $\eta_{\mathrm{T,L}}(\gamma)$ are positive, irrespectively of the Lorentz factor $\gamma \geqslant 1$, and related to the cutoff frequencies in (4.3) by $\omega_{\mathrm{T,L,max}}(\gamma) = m_{\mathrm{t}}\sqrt{\eta_{\mathrm{T,L}}}$.

5. Tachyonic Cherenkov densities averaged with relativistic electron distributions

We rescale the frequency in the radiation densities (4.5), $\hat{\omega} = \sqrt{\varepsilon\mu_0}\omega/m_{\mathrm{t}}$,

$$p^{\mathrm{T}}(\omega,\gamma) = \frac{\mu m_{\mathrm{t}}}{\sqrt{\varepsilon\mu_0}} \frac{\alpha_q(\omega)\hat{\omega}}{\hat{\omega}^2+1} \times \bigg[\bigg(1 - \bigg(\frac{1}{\varepsilon\mu} - 1\bigg)\hat{\omega}^2\bigg)\gamma^2 - \big(\hat{\omega}^2+1\big)\bigg] \times \frac{1}{\gamma\sqrt{\gamma^2-1}},$$

$$p^{\mathrm{L}}(\omega,\gamma) = \frac{m_{\mathrm{t}}}{\varepsilon\sqrt{\varepsilon\mu_0}} \frac{\alpha_q(\omega)\hat{\omega}}{\hat{\omega}^2+1} \frac{\gamma}{\sqrt{\gamma^2-1}}, \tag{5.1}$$

where we have introduced the frequency-dependent tachyonic fine-structure constant $\alpha_q(\omega) = q^2/(4\pi\Omega^2(\omega))$. The scale factor $\Omega^2(\omega)$, cf. after (2.5), is chosen as

$$\Omega^2(\omega) = \bigg(\frac{\hat{\omega}^2}{\hat{\omega}^2+1}\bigg)^{\sigma}, \tag{5.2}$$

where the exponent σ is to be determined from an empirical spectral fit. We note $\Omega(\omega) \to 1$ for $\omega \to \infty$ as well as $m_{\mathrm{t}} \to 0$, and $\Omega(\omega \to 0) \sim \hat{\omega}^{\sigma}$. The permeabilities $\varepsilon,\mu,\varepsilon_0,\mu_0$ are positive and constant, satisfying $\varepsilon\mu \leqslant 1$ and $\varepsilon_0\mu_0 \leqslant 1$, cf. after (4.6). The transversal/longitudinal spectral range is $0 \leqslant \omega \leqslant \omega_{\mathrm{T,L,max}}(\gamma)$, with $\omega_{\mathrm{T,L,max}} = m_{\mathrm{t}}\sqrt{\eta_{\mathrm{T,L}}(\gamma)}$. The cutoff factors $\eta_{\mathrm{T,L}}(\gamma)$ in (4.6) are monotonically increasing, from zero at $\gamma = 1$ to the maximum $\eta_{\mathrm{T}}(\infty) = [\varepsilon\mu_0(1/(\varepsilon\mu) - 1)]^{-1}$ and $\eta_{\mathrm{L}}(\infty) = [\varepsilon\mu_0(1/(\varepsilon_0\mu_0) - 1)]^{-1}$, respectively.

We average the radiation densities (5.1) with an electronic power-law distribution [16–19],

$$\mathrm{d}\rho_{\alpha,\beta}(\gamma) = A_{\alpha,\beta}\gamma^{-\alpha-1}\mathrm{e}^{-\beta\gamma}\sqrt{\gamma^2-1}\,\mathrm{d}\gamma, \tag{5.3}$$

where the dimensionless normalization constant $A_{\alpha,\beta}$ is related to the electronic number count N_e by

$$N_\mathrm{e} = A_{\alpha,\beta}K_{\alpha,\beta}, \qquad K_{\alpha,\beta} = \int_1^\infty \gamma^{-\alpha-1}\mathrm{e}^{-\beta\gamma}\sqrt{\gamma^2-1}\,\mathrm{d}\gamma. \tag{5.4}$$

The exponential cutoff $\beta = m_\mathrm{e}/(k_\mathrm{B}T)$ determines the electron temperature, $T[\mathrm{K}] \approx 5.93\times 10^9/\beta$. k_B is the Boltzmann constant and m_e the electron mass. A thermal Maxwell–Boltzmann distribution requires the electron index $\alpha = -2$.

The spectral average of the transversal radiation densities in (5.1) is carried out as

$$\big\langle p^\mathrm{T}(\omega)\big\rangle_{\alpha,\beta} = \int_1^\infty p^\mathrm{T}(\omega,\gamma)\theta\big(\omega_{\mathrm{T,max}}(\gamma)-\omega\big)\,\mathrm{d}\rho_{\alpha,\beta}(\gamma), \tag{5.5}$$

where θ is the Heaviside step function. The same applies to the longitudinal density, if we replace $\mathrm{T}\to\mathrm{L}$ and $\varepsilon\mu\to\varepsilon_0\mu_0$. To evaluate integral (5.5), we solve the inequality $\omega < \omega_{\mathrm{T,max}}$, $\omega_{\mathrm{T,max}} = m_\mathrm{t}\sqrt{\eta_\mathrm{T}(\gamma)}$, for γ, cf. (4.6):

$$\gamma^2 > \gamma^2_{\mathrm{T,min}}(\omega) = \frac{1+\hat\omega^2}{1+\hat\omega^2(1-1/(\varepsilon\mu))}, \tag{5.6}$$

which is valid if the denominator is positive. As pointed out after (5.2), only frequencies in the range $0<\omega<\omega_{\mathrm{T,max}}(\infty)$ can be radiated, where $\omega_{\mathrm{T,max}}(\infty) = m_\mathrm{t}\sqrt{\eta_\mathrm{T}(\infty)}$. In this frequency range, the denominator in (5.6) is positive and $\gamma_{\mathrm{T,min}}(\omega)$ is monotonically increasing, reaching infinity at $\omega_{\mathrm{T,max}}(\infty)$. Thus, for a frequency in the range $0<\omega<\omega_{\mathrm{T,max}}(\infty)$ to be radiated, this requires the electronic Lorentz factor γ to exceed $\gamma_{\mathrm{T,min}}(\omega)$. This holds true for longitudinal radiation as well, if we perform the substitutions $\mathrm{T}\to\mathrm{L}$ and $\varepsilon\mu\to\varepsilon_0\mu_0$, which also define $\gamma_{\mathrm{L,min}}(\omega)$ via (5.6).

With these prerequisites, the average (5.5) can be reduced to the spectral functions [20]

$$B^{\mathrm{T,L}}(\omega,\gamma_1) = \int_{\gamma_1}^\infty p^{\mathrm{T,L}}(\omega,\gamma)\,\mathrm{d}\rho_{\alpha,\beta}(\gamma), \tag{5.7}$$

so that, cf. (5.6),

$$\big\langle p^\mathrm{T}(\omega)\big\rangle_{\alpha,\beta} = \theta\big(\omega_{\mathrm{T,max}}(\infty)-\omega\big)B^\mathrm{T}\big(\omega,\gamma_{\mathrm{T,min}}(\omega)\big). \tag{5.8}$$

In the Heaviside function θ, it is convenient to rescale the argument, writing $\theta(\hat\omega_{\mathrm{T,max}}(\infty)-\hat\omega)$, where $\hat\omega_{\mathrm{T,max}}(\infty) = (1/(\varepsilon\mu)-1)^{-1/2}$. The longitudinal average $\langle p^\mathrm{L}(\omega)\rangle_{\alpha,\beta}$ is obtained by the substitutions $\mathrm{T}\to\mathrm{L}$ and $\varepsilon\mu\to\varepsilon_0\mu_0$ in (5.6) and (5.8).

The spectral functions $B^{\mathrm{T,L}}(\omega,\gamma_1)$ in (5.7) admit integration in terms of incomplete gamma functions,

$$\begin{aligned} B^\mathrm{T}(\omega,\gamma_1) = A_{\alpha,\beta}&\frac{\mu m_\mathrm{t}}{\sqrt{\varepsilon\mu_0}}\frac{\alpha_q\hat\omega}{\hat\omega^2+1}\frac{1}{\beta^2\gamma_1^{\alpha+1}}\\ &\times\bigg\{\bigg[\alpha(\alpha+1)\bigg(1-\bigg(\frac{1}{\varepsilon\mu}-1\bigg)\hat\omega^2\bigg)-\beta^2\big(\hat\omega^2+1\big)\bigg]\\ &\times(\beta\gamma_1)^{\alpha+1}\Gamma(-1-\alpha,\beta\gamma_1)\\ &+\bigg(1-\bigg(\frac{1}{\varepsilon\mu}-1\bigg)\hat\omega^2\bigg)\mathrm{e}^{-\beta\gamma_1}(\beta\gamma_1-\alpha)\bigg\}, \end{aligned} \tag{5.9}$$

where $\alpha_q(\omega)$ is the tachyonic fine-structure constant defined before (5.2). The longitudinal spectral function reads

$$\begin{aligned} B^\mathrm{L}(\omega,\gamma_1) = A_{\alpha,\beta}&\frac{m_\mathrm{t}}{\varepsilon\sqrt{\varepsilon\mu_0}}\frac{\alpha_q\hat\omega}{\hat\omega^2+1}\frac{1}{\beta^2\gamma_1^{\alpha+1}}\\ &\times\big[\alpha(\alpha+1)(\beta\gamma_1)^{\alpha+1}\Gamma(-\alpha-1,\beta\gamma_1)\\ &+\mathrm{e}^{-\beta\gamma_1}(\beta\gamma_1-\alpha)\big]. \end{aligned} \tag{5.10}$$

We note that Γ is elementary for Maxwell–Boltzmann averages, $\alpha=-2$, $\Gamma(1,\beta\gamma_1) = \mathrm{e}^{-\beta\gamma_1}$, and it decays exponentially for $\beta\gamma_1\gg 1$, $\Gamma(-\alpha-1,\beta\gamma_1)\sim(\beta\gamma_1)^{-\alpha-2}\mathrm{e}^{-\beta\gamma_1}$. Accordingly, $B^\mathrm{T}(\omega,\gamma_{\mathrm{T,min}}(\omega))$ decays exponentially as well, since $\gamma_{\mathrm{T,min}}(\omega)$ diverges for $\omega\to\omega_{\mathrm{T,max}}(\infty)$, cf. (5.6), and the same holds true for $B^\mathrm{L}(\omega,\gamma_{\mathrm{L,min}}(\omega))$ and $\omega\to\omega_{\mathrm{L,max}}(\infty)$. In the low-frequency limit, $\hat\omega\to 0$, we find $B^{\mathrm{T,L}}(\omega,\gamma_{\mathrm{T,L,min}}(\omega))\propto\hat\omega^{1-2\sigma}$, cf. (5.2).

6. Tachyonic spectral fit to Jupiter's radio emission

6.1. Superluminal Cherenkov flux in the radio band

We restore the units $\hbar = c = 1$ and use eV units for the tachyon mass, so that m_t stands for $m_\mathrm{t}c^2[\mathrm{eV}]$. As for the radiated frequencies, we put $\omega = h[\mathrm{eV\,s}]\nu[\mathrm{Hz}]$, where $h[\mathrm{eV\,s}]\approx 2\pi\times 6.582\times 10^{-16}$. The energy-dependent tachyonic fine-structure constant is dimensionless, $\alpha_q(\omega) = \alpha_\mathrm{t}/\Omega^2(\omega)$, cf. (5.2); the proportionality factor $\alpha_\mathrm{t} = q^2/(4\pi\hbar c)$ is the tachyonic counterpart to the electric fine-structure constant $e^2/(4\pi\hbar c)$, $\alpha_q(\omega\to\infty) = \alpha_\mathrm{t}$. The permeabilities (2.1) and the temperature parameter β are dimensionless. The spectral functions $B^{\mathrm{T,L}}$ in (5.9) and (5.10) and the averaged densities $\langle p^{\mathrm{T,L}}(\omega)\rangle_{\alpha,\beta}$ in (5.8) are in eV units accordingly. The power transversally and longitudinally radiated is thus $P^{\mathrm{T,L}}[\mathrm{eV/s}] = \int\langle p^{\mathrm{T,L}}(\omega)\rangle_{\alpha,\beta}\,\mathrm{d}\nu$, where we substitute $m_\mathrm{t}\to m_\mathrm{t}c^2[\mathrm{eV}]$ and $\omega\to h[\mathrm{eV\,s}]\nu$ in the integrand. The transversal/longitudinal flux densities read

$$\begin{aligned} F_\nu^{\mathrm{T,L}}\big[\mathrm{eV/cm^2}\big] &= \frac{1}{4\pi d^2[\mathrm{cm}]}\frac{\mathrm{d}P^{\mathrm{T,L}}}{\mathrm{d}\nu}\big[\mathrm{eV\,s^{-1}\,Hz^{-1}}\big]\\ &= \frac{\langle p^{\mathrm{T,L}}(\omega)\rangle_{\alpha,\beta}[\mathrm{eV}]}{4\pi d^2[\mathrm{cm}]}, \end{aligned} \tag{6.1}$$

where $d[\mathrm{cm}]$ is the distance to the radiating source. The total unpolarized flux density is $F_\nu^{\mathrm{T+L}} = F_\nu^\mathrm{T} + F_\nu^\mathrm{L}$. Jupiter's standard geocentric distance is $d\approx 4.04$ AU $\approx 6.04\times 10^{13}$ cm [1,2,21]. As we have already expressed $\langle p^{\mathrm{T,L}}(\omega)\rangle_{\alpha,\beta}$ in terms of the rescaled frequency $\hat\omega = \sqrt{\varepsilon\mu_0}\omega/m_\mathrm{t}$, we only need to substitute $\hat\omega\to\kappa_{\mathrm{t,Hz}}\nu$ in the spectral densities (5.8), where ν is measured in hertz, and $\kappa_{\mathrm{t,Hz}}[\mathrm{s}]$ is a fitting parameter, $\kappa_{\mathrm{t,Hz}} = \sqrt{\varepsilon\mu_0}h[\mathrm{eV\,s}]/(m_\mathrm{t}c^2[\mathrm{eV}])$, determining the tachyon mass in the radio band.

We note the conversions $\nu[\mathrm{GHz}]\approx 2.418\times 10^5 E[\mathrm{eV}]$ and $1\ \mathrm{Jy}\approx 6.2415\times 10^{-12}\ \mathrm{eV/(cm^2)}$ [21], so that $F_\nu^{\mathrm{T,L}}[\mathrm{Jy}]\approx 1.6022\times 10^{11}F_\nu^{\mathrm{T,L}}[\mathrm{eV/cm^2}]$. To better distinguish linear spectral slopes from curved spectral cutoffs, one can use the rescaled flux density $\nu^k F_\nu^{\mathrm{T,L}}[\mathrm{Jy\,(GHz)}^k]$, where k is preferably a positive integer exponent. In Fig. 1, we plot $\nu F_\nu^{\mathrm{T,L}}[\mathrm{Jy\,GHz}]$ against $\nu[\mathrm{GHz}]$, and the fit is performed with the total flux density $\nu F_\nu^{\mathrm{T+L}} = \nu(F_\nu^\mathrm{T}+F_\nu^\mathrm{L})[\mathrm{Jy\,GHz}]$.

Summarizing the flux densities employed in the spectral fit in Fig. 1, we assemble $\nu^k F_\nu^{\mathrm{T,L}}$ in the above stated units. The transversal Cherenkov density (6.1) reads

$$\begin{aligned} \nu^k F_\nu^\mathrm{T}\big[\mathrm{Jy(GHz)}^k\big] = \frac{1.6022\times 10^{11}}{4\pi d^2[\mathrm{cm}]}&\nu^k\theta\big(\hat\omega_{\mathrm{T,max}}(\infty)-\hat\omega\big)\\ &\times B^\mathrm{T}\big(\omega,\gamma_{\mathrm{T,min}}(\omega)\big), \end{aligned} \tag{6.2}$$

where $\hat\omega_{\mathrm{T,max}}(\infty) = (1/(\varepsilon\mu)-1)^{-1/2}$, cf. after (5.8). The spectral function B^T in (5.9) and the argument $\gamma_{\mathrm{T,min}}(\omega)$ in (5.6) are already expressed in the rescaled variable $\hat\omega = \sqrt{\varepsilon\mu_0}\omega/m_\mathrm{t}$. The longitudinal counterpart to (6.2) is obtained by replacing $\mathrm{T}\to\mathrm{L}$ and $\varepsilon\mu\to\varepsilon_0\mu_0$, so that $\hat\omega_{\mathrm{L,max}}(\infty) = (1/(\varepsilon_0\mu_0)-1)^{-1/2}$.

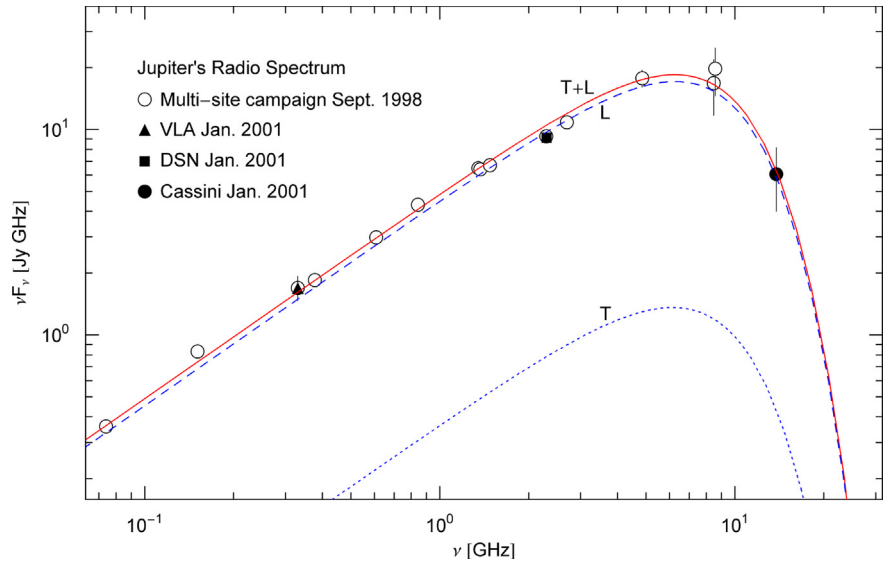

Fig. 1. Tachyonic Cherenkov fit to the Jovian radio emission. Data points of the 1998 multi-site campaign from [2], VLA (Very Large Array), DSN (Deep Space Network) and Cassini 2001 data from [1]. The fit T + L (solid curve) depicts the total tachyonic flux density $\nu F_\nu^{\mathrm{T+L}}$ rescaled with frequency. This unpolarized density is obtained by adding the transversal flux component νF_ν^{T} (dotted curve labeled T) and the longitudinal component νF_ν^{L} (dashed curve L), generated by a thermal electron plasma, cf. (6.2). Jupiter's radio spectrum shows an extended power-law ascent terminating in a spectral peak around 6 GHz, which is followed by an exponentially decaying tail inferred from the Cassini data point at 13.8 GHz. The fitting parameters are recorded in Section 6.2.

In (6.2), we substitute $\hat{\omega} = \kappa_{\mathrm{t}}\nu$, where the frequency ν is measured in GHz so that $\kappa_{\mathrm{t}} = 10^9\kappa_{\mathrm{t,Hz}}$ or, cf. after (6.1),

$$\kappa_{\mathrm{t}}[\mathrm{s}] = 10^9\frac{\sqrt{\varepsilon\mu_0}h[\mathrm{eV\,s}]}{m_{\mathrm{t}}c^2[\mathrm{eV}]} \approx 4.136\times 10^{-6}\frac{\sqrt{\varepsilon\mu_0}}{m_{\mathrm{t}}c^2[\mathrm{eV}]}. \tag{6.3}$$

In this parametrization, we find the transversal spectral function (5.9) as

$$\begin{aligned} B^{\mathrm{T}}(\omega,\gamma_{\mathrm{T,min}}) = {} & A_{\alpha,\beta}m_{\mathrm{t}}c^2[\mathrm{eV}]\frac{\alpha_{\mathrm{t}}}{\varepsilon\sqrt{\varepsilon\mu_0}}\frac{\varepsilon\mu}{\Omega^2(\nu)}\frac{\kappa_{\mathrm{t}}\nu}{\kappa_{\mathrm{t}}^2\nu^2+1}\frac{1}{\beta^2\gamma_{\mathrm{T,min}}^{\alpha+1}} \\ & \times\Big\{\Big[\alpha(\alpha+1)\Big(1-\Big(\frac{1}{\varepsilon\mu}-1\Big)\kappa_{\mathrm{t}}^2\nu^2\Big) \\ & -\beta^2\big(\kappa_{\mathrm{t}}^2\nu^2+1\big)\Big](\beta\gamma_{\mathrm{T,min}})^{\alpha+1} \\ & \times\Gamma(-1-\alpha,\beta\gamma_{\mathrm{T,min}}) \\ & +\Big(1-\Big(\frac{1}{\varepsilon\mu}-1\Big)\kappa_{\mathrm{t}}^2\nu^2\Big) \\ & \times \mathrm{e}^{-\beta\gamma_{\mathrm{T,min}}}(\beta\gamma_{\mathrm{T,min}}-\alpha)\Big\}, \end{aligned} \tag{6.4}$$

and the longitudinal spectral function in (5.10) reads

$$\begin{aligned} B^{\mathrm{L}}(\omega,\gamma_{\mathrm{L,min}}) = {} & A_{\alpha,\beta}m_{\mathrm{t}}c^2[\mathrm{eV}]\frac{\alpha_{\mathrm{t}}}{\varepsilon\sqrt{\varepsilon\mu_0}}\frac{1}{\Omega^2(\nu)}\frac{\kappa_{\mathrm{t}}\nu}{\kappa_{\mathrm{t}}^2\nu^2+1}\frac{1}{\beta^2\gamma_{\mathrm{L,min}}^{\alpha+1}} \\ & \times\big[\alpha(\alpha+1)(\beta\gamma_{\mathrm{L,min}})^{\alpha+1}\Gamma(-\alpha-1,\beta\gamma_{\mathrm{L,min}}) \\ & +\mathrm{e}^{-\beta\gamma_{\mathrm{L,min}}}(\beta\gamma_{\mathrm{L,min}}-\alpha)\big]. \end{aligned} \tag{6.5}$$

In (6.4) and (6.5), we have to insert the frequency-dependent minimal Lorentz factors, cf. (5.6),

$$\begin{aligned} \gamma_{\mathrm{T,min}}(\nu) &= \frac{\sqrt{1+\kappa_{\mathrm{t}}^2\nu^2}}{\sqrt{1+\kappa_{\mathrm{t}}^2\nu^2(1-1/(\varepsilon\mu))}}, \\ \gamma_{\mathrm{L,min}}(\nu) &= \frac{\sqrt{1+\kappa_{\mathrm{t}}^2\nu^2}}{\sqrt{1+\kappa_{\mathrm{t}}^2\nu^2(1-1/(\varepsilon_0\mu_0))}}, \end{aligned} \tag{6.6}$$

and the scale factor

$$\Omega^2(\nu) = \Big(\frac{\kappa_{\mathrm{t}}^2\nu^2}{\kappa_{\mathrm{t}}^2\nu^2+1}\Big)^{\sigma} \tag{6.7}$$

of the tachyonic fine-structure constant $\alpha_q(\omega) = \alpha_{\mathrm{t}}/\Omega^2$, $\alpha_{\mathrm{t}} = q^2/(4\pi\hbar c)$, see (5.2) and before (6.1).

The Heaviside function in the flux density (6.2) can be replaced by $\theta(\hat{\omega}_{\mathrm{L,T,max}}(\infty)-\kappa_{\mathrm{t}}\nu)$. The highest frequency transversally/longitudinally radiated is $\nu_{\mathrm{T,max}} = (1/(\varepsilon\mu)-1)^{-1/2}/\kappa_{\mathrm{t}}$ and $\nu_{\mathrm{L,max}} = (1/(\varepsilon_0\mu_0)-1)^{-1/2}/\kappa_{\mathrm{t}}$ respectively, cf. after (6.2). The tachyonic mass parameter κ_{t} is defined in (6.3). The constant amplitudes in (6.2) and (6.4) can be combined to one fitting parameter,

$$a_{\mathrm{t}} = \frac{1.6022\times 10^{11}}{4\pi d^2[\mathrm{cm}]}m_{\mathrm{t}}c^2[\mathrm{eV}]A_{\alpha,\beta}\frac{\alpha_{\mathrm{t}}}{\varepsilon\sqrt{\varepsilon\mu_0}}, \tag{6.8}$$

with $4\pi d^2 \approx 4.58\times 10^{28}$ cm^2 for Jupiter, cf. after (6.1). This amplitude a_{t} can also be used for the longitudinal radiation component in (6.2) and (6.5).

6.2. Spectral asymptotics and tachyonic Cherenkov fit of the Jovian radio emission

We consider a thermal electron distribution (5.3) with electron index $\alpha = -2$, and permeabilities (2.1) satisfying $\varepsilon\mu = \varepsilon_0\mu_0 = 1$. (This is slightly more general than vacuum permeabilities $\varepsilon = \mu = 1$, $\varepsilon_0 = \mu_0 = 1$.) The transversal spectral function $B^{\mathrm{T}}(\omega,\gamma_{\mathrm{T,min}})$ in (6.4) then simplifies to

$$\begin{aligned} B^{\mathrm{T}}(\omega,\gamma_{\mathrm{T,min}}) = {} & A_{\alpha,\beta}m_{\mathrm{t}}c^2[\mathrm{eV}] \\ & \times\frac{\alpha_{\mathrm{t}}}{\varepsilon\sqrt{\varepsilon\mu_0}}\frac{1}{\Omega^2(\nu)}\frac{\kappa_{\mathrm{t}}\nu}{\kappa_{\mathrm{t}}^2\nu^2+1}\frac{\gamma_{\mathrm{T,min}}}{\beta^2}\mathrm{e}^{-\beta\gamma_{\mathrm{T,min}}} \\ & \times\Big[\big(2-\beta^2\big(\kappa_{\mathrm{t}}^2\nu^2+1\big)\big)\frac{1}{\beta\gamma_{\mathrm{T,min}}} \\ & +2+\beta\gamma_{\mathrm{T,min}}\Big], \end{aligned} \tag{6.9}$$

and its longitudinal counterpart in (6.5) is

$$B^{\mathrm{L}}(\omega,\gamma_{\mathrm{L,min}}) = A_{\alpha,\beta} m_{\mathrm{t}} c^2[\mathrm{eV}] \frac{\alpha_{\mathrm{t}}}{\varepsilon\sqrt{\varepsilon\mu_0}} \frac{1}{\Omega^2(\nu)} \frac{\kappa_{\mathrm{t}}\nu}{\kappa_{\mathrm{t}}^2\nu^2+1} \frac{\gamma_{\mathrm{L,min}}}{\beta^2} \times \mathrm{e}^{-\beta\gamma_{\mathrm{L,min}}}\left(\frac{2}{\beta\gamma_{\mathrm{L,min}}}+2+\beta\gamma_{\mathrm{L,min}}\right). \quad (6.10)$$

The minimal Lorentz factor to be substituted is $\gamma_{\mathrm{T,L,min}}(\nu) = \sqrt{1+\kappa_{\mathrm{t}}^2\nu^2}$, cf. (6.6), and the fine-structure scale factor $\Omega^2(\nu)$ is stated in (6.7). ν is measured in GHz, and the tachyonic mass parameter κ_{t} is defined in (6.3).

The flux densities $\nu^k F_\nu^{\mathrm{T,L}}$ in (6.2) apply, with the Heaviside function dropped. In the low-frequency limit $\kappa_{\mathrm{t}}\nu \to 0$, we find the unpolarized flux

$$\nu F_\nu^{\mathrm{T+L}} \sim A_0 \nu^{2-2\sigma}, \qquad A_0 = \frac{a_{\mathrm{t}}\kappa_{\mathrm{t}}^{1-2\sigma}}{\beta^3}\mathrm{e}^{-\beta}(2+\beta)^2. \quad (6.11)$$

The parameter a_{t} is defined in (6.8). We can estimate the amplitude A_0 and the exponent σ by fitting this power-law slope, which is linear in a log–log plot, to the low-frequency spectrum. In the asymptotic high-frequency limit $\kappa_{\mathrm{t}}\nu \gg 1$, the unpolarized flux reads

$$\nu F_\nu^{\mathrm{T+L}} \sim A_\infty \mathrm{e}^{-\rho\nu}(2+\rho\nu)^2, \quad A_\infty = \frac{a_{\mathrm{t}}}{\beta^3\kappa_{\mathrm{t}}}, \quad \rho = \beta\kappa_{\mathrm{t}}. \quad (6.12)$$

An initial estimate of A_∞ and ρ is obtained by fitting this exponentially decaying flux in the high-frequency regime. Once the parameters $A_{0,\infty}$, σ and ρ have been estimated from the asymptotic spectral fits, we find the temperature parameter β of the radiating electron population by solving

$$\frac{A_0}{A_\infty}\rho^{2\sigma-2} = \beta^{2\sigma-2}\mathrm{e}^{-\beta}(2+\beta)^2. \quad (6.13)$$

This equation readily follows from the definition of the asymptotic fitting parameters $A_{0,\infty}$ and ρ in (6.11) and (6.12). Initial values for κ_{t} and a_{t} are found as $\kappa_{\mathrm{t}} = \rho/\beta$ and $a_{\mathrm{t}} = A_\infty\beta^2\rho$.

The least-squares fit of the flux densities (6.2) is performed by varying the parameters $A_{0,\infty}$, ρ and σ in the vicinity of their initial values obtained from the asymptotic fits (6.11) and (6.12); the corresponding β is obtained by solving (6.13). In addition, we may vary the permeabilities in the vicinity of $\varepsilon\mu = \varepsilon_0\mu_0 = 1$, subject to the constraints $\varepsilon\mu \leqslant 1$ and $\varepsilon_0\mu_0 \leqslant 1$, cf. after (4.6). The electron index can also be varied around its equilibrium value $\alpha = -2$, cf. (5.3), by employing the nonthermal spectral functions (6.4) and (6.5) instead of (6.9) and (6.10), but this is not necessary for the Jovian radio spectrum.

The tachyonic Cherenkov fit of Jupiter's radio emission depicted in Fig. 1 is performed with a thermal electron distribution $\alpha = -2$ and permeabilities $\varepsilon\mu = \varepsilon_0\mu_0 = 1$. The numerical values of the fitting parameters are

$$\sigma \approx 0.5, \qquad \beta \approx 23.6, \qquad \kappa_{\mathrm{t}} \approx 0.0339, \qquad a_{\mathrm{t}} \approx 1.78\times 10^{12}. \quad (6.14)$$

The fine-structure scaling exponent σ is defined in (6.7), the temperature parameter β in (5.3), the tachyonic mass parameter κ_{t}[s] in (6.3), and the flux amplitude a_{t}[eV/cm^2] in (6.8). In practice, we use the parameters of the asymptotic flux limits (6.11) and (6.12) as fitting parameters, which are $A_0 \approx 4.9$, $A_\infty \approx 4.0\times 10^9$, $\sigma \approx 0.5$ and $\rho \approx 0.8$. The parameters in (6.14) have been calculated from these values as explained above.

The electron temperature is $T[\mathrm{K}] \approx 2.51\times 10^8$, cf. after (5.4), which is the only point where the electron mass enters, via $\beta = m_{\mathrm{e}}/(k_{\mathrm{B}}T)$. (The mass of the radiating particle does not show in the classical Cherenkov densities (4.5), in contrast to the tachyon mass m_{t}.) Assuming vacuum permeabilities, $\varepsilon \approx \mu \approx 1$, $\varepsilon_0 \approx \mu_0 \approx 1$, we can estimate the tachyon mass in the radio band, $m_{\mathrm{t}}c^2[\mathrm{eV}] \approx 1.22\times 10^{-4}$ or $m_{\mathrm{t}}c^2 \approx 29.5$ GHz, cf. (6.3) and (6.14). From the amplitude a_{t} in (6.8) and the Jovian distance estimate, we find the product of the asymptotic tachyonic fine-structure constant α_{t} (defined before (6.1)) and the normalization factor of the electron distribution (5.3) as $A_{\alpha,\beta}\alpha_{\mathrm{t}} \approx 4.17\times 10^{33}$. The integral $K_{\alpha,\beta}$ in (5.4) determining the electron number $N_{\mathrm{e}} = A_{\alpha,\beta}K_{\alpha,\beta}$ is calculated with the temperature parameter β in (6.14), $K_{\alpha=-2,\beta} \approx 6.65\times 10^{-13}$. The estimate for the product of electron count and tachyonic fine-structure constant is thus $N_{\mathrm{e}}\alpha_{\mathrm{t}} \approx 2.77\times 10^{21}$.

7. Conclusion

We have investigated the emission of tachyonic radiation modes by freely propagating electrons in a dispersive spacetime. The superluminal group velocity $\upsilon_{\mathrm{T,L}} = \mathrm{d}\omega/\mathrm{d}k_{\mathrm{T,L}}(\omega)$ is caused by the negative mass-square in the wave numbers (3.2) of the tachyonic radiation field. $\upsilon_{\mathrm{T,L}}$ differs for transversal and longitudinal modes [14], unless the wave numbers coincide, which requires permeabilities satisfying $\varepsilon_0\mu_0 = \varepsilon\mu$. The tachyonic wavelength is $\lambda_{\mathrm{T,L}} = 2\pi/k_{\mathrm{T,L}}$. In the radio band and with vacuum permeabilities, we find the group velocity $\upsilon_{\mathrm{T,L}}/c = \sqrt{\nu^2+m_{\mathrm{t}}^2}/\nu$ and wavelength $\lambda_{\mathrm{T,L}}[\mathrm{cm}] \approx 29.98/\sqrt{\nu^2+m_{\mathrm{t}}^2}$, with ν in GHz. A tachyon mass m_{t} of 29.5 GHz is inferred from the spectral fit in Fig. 1, cf. after (6.14).

We introduced tachyonic field strengths and inductions defined by constitutive relations with frequency-dependent permeabilities. We then developed an equivalent 4D space–frequency representation of the dispersive radiation field, deriving manifestly covariant field equations. Thus the suggestive and efficient formalism of manifest covariance can be maintained, but the underlying space conception is non-relativistic, as superluminal wave propagation requires an absolute spacetime conception to preserve causality [8–10].

We focused on superluminal Cherenkov radiation, the tachyonic radiation field being generated by a classical subluminal charge uniformly moving in a permeable spacetime. The electron mass does not enter in the classical radiation densities (4.4), which suggests that the tachyonic quanta are actually emitted by the medium stimulated by the field of the moving electron [3,22]. A longitudinal radiation component emerges, with amplitude proportional to the negative mass-square of the tachyonic modes. We parametrized the Cherenkov flux densities with the Lorentz factor of the inertial charge, averaged them with a relativistic electron distribution, and explained how to perform tachyonic spectral fits in the radio band.

A flux average over a mildly relativistic thermal electron population (with Maxwell–Boltzmann distribution) suffices to model the currently observed Jovian radio spectrum. We also calculated the tachyonic Cherenkov flux radiated by nonthermal electron populations (with power-law distribution), cf. Section 5, which can be useful to model X- and γ-ray spectra [23–25]. As for Jupiter, the low flux density at 13.8 GHz (Cassini 2001 in-situ measurement [1,26]) is caused by an exponential spectral cutoff. The low-frequency spectrum is linear in the double-logarithmic flux representation of Fig. 1. The cross-over region around the spectral peak at 6 GHz is also well reproduced by the tachyonic flux densities (4.4) averaged over a thermal electron population.

References

[1] S.J. Bolton, et al., Nature 415 (2002) 987.
[2] I. de Pater, et al., Icarus 163 (2003) 434.
[3] L.D. Landau, E.M. Lifshitz, Electrodynamics of Continuous Media, Pergamon, Oxford, 1984.

[4] V.L. Ginzburg, V.N. Tsytovich, Transition Radiation and Transition Scattering, Hilger, Bristol, 1990.
[5] B.M. Bolotovskiĭ, V.L. Ginzburg, Sov. Phys. Usp. 15 (1972) 184.
[6] G.N. Afanasiev, M.V. Lyubchenko, Yu.P. Stepanovsky, Proc. R. Soc. A, Math. Phys. Eng. Sci. 462 (2006) 689.
[7] R. Tomaschitz, Phys. Lett. A 377 (2013) 945.
[8] R. Tomaschitz, Europhys. Lett. 97 (2012) 39003.
[9] R. Tomaschitz, Europhys. Lett. 98 (2012) 19001.
[10] R. Tomaschitz, Europhys. Lett. 102 (2013) 61002.
[11] R. Tomaschitz, Eur. Phys. J. C 69 (2010) 241.
[12] R. Tomaschitz, Physica A 320 (2003) 329.
[13] R. Tomaschitz, Opt. Commun. 282 (2009) 1710.
[14] R. Tomaschitz, Physica B 404 (2009) 1383.
[15] R. Tomaschitz, Appl. Phys. B 101 (2010) 143.
[16] R. Tomaschitz, Physica A 385 (2007) 558.
[17] R. Tomaschitz, Physica A 387 (2008) 3480.
[18] R. Tomaschitz, Physica B 405 (2010) 1022.
[19] R. Tomaschitz, Physica A (2013), http://dx.doi.org/10.1016/j.physa.2013.09.068.
[20] R. Tomaschitz, Ann. Phys. 322 (2007) 677.
[21] K. Nakamura, et al., J. Phys. G 37 (2010) 075021.
[22] R. Tomaschitz, Class. Quantum Grav. 18 (2001) 4395.
[23] A. Bhardwaj, et al., J. Geophys. Res. 111 (2006) A11225.
[24] G. Branduardi-Raymont, et al., Astron. Astrophys. 463 (2007) 761.
[25] G. Branduardi-Raymont, et al., Planet. Space Sci. 55 (2007) 1126.
[26] J.L. Kloosterman, et al., Icarus 193 (2008) 644.